Hydrophobic polyampholytes and non-freezing cold temperature stimulate internalization of Au nanoparticles to zwitterionic liposomes

Sana Ahmed, Kazuaki Matsumura[*] and Tsutomu Hamada[*]

School of Materials Science, Japan Advanced Institute of Science and Technology, Nomi, Ishikawa 923-1292, Japan

*Corresponding authors

KEYWORDS: Nanoparticle internalization, Hydrophobic polyampholytes, Cold temperature, Cell-sized liposomes

ABSTRACT

Nanomedicine relies on the effective internalization of nanoparticles combined with polymeric nanocarriers into living cells. Thus, exploration of internalization is essential for improving the efficacy of nanoparticle-based strategies in clinical practice. Here, we investigated the physicochemical internalization of gold nanoparticles (AuNPs) conjugated with hydrophobic polyampholytes into cell-sized liposomes at a low but non-frozen temperature. The hydrophobic polyampholytes localized in the disordered phase of the membrane, and internalization of AuNPs was enhanced in the presence of hydrophobic polyampholytes together with incubation at –3°C as compared to 25°C. These results contribute toward a mechanistic understanding for developing a model nanomaterials-driven delivery system based on hydrophobic polyampholytes and low temperature.

1. INTRODUCTION

Several strategies are actively being developed to effectively deliver materials inside cells for various therapeutic applications. The most popular approaches currently include electroporation[1], ultra-sonication[2], and cell-penetrating peptides[3] to promote the diffusion of target molecules across the cell membrane. However, there are major drawbacks associated with these strategies since the processes often result in permanent cell or tissue damage. Therefore, a great challenge remains in finding effective strategies to transport a molecule across the cell membrane.

There has been some success in the use of various carriers such as liposomes[4], micelles[5], nanogels[6], and other polysaccharides-based nanocarriers[7] for carrying proteins inside cells. However, several of the carriers developed to date show instability[8] and/or high toxicity[9]. Recently, hydrophobic polyampholytes have attracted substantial research attention as candidate carriers because of their stability, low toxicity, and small size.[10] Polyampholytes including zwitterionic polymers also show promise in several other biomedical applications such as for cell preservation[11], anti-biofouling[12], and tissue engineering.[13,14] These polyelectrolytes contain both cationic and anionic charges in the polymeric backbone. We previously developed new hydrophobic polyampholytes that can form self-assembled nanoparticles and efficiently transfer protein-based materials to the cytosol of cells.[15-19] These hydrophobic polyampholytes were easily designed by modifying the anionic functional group dodecylsuccinic anhydride (DDSA) and a large amount of succinic anhydride (SA) in ε-poly-L-lysine (PLL), which confers the hydrophobic polyampholytes with an anionic charge. Although hydrophobicity can enhance cell membrane affinity, it is nevertheless difficult to internalize proteins inside cells because of the negatively charged surface potential. Thus, to achieve efficient delivery to cells, we also developed a novel low temperature-based freeze-concentration approach to act as a driving force to internalize materials inside cells

efficiently.[15-19] Freeze concentration is a physicochemical phenomenon wherein water molecules are crystallized into ice so that the solutes present in the system are ejected, which thereby enhances the concentration. The increased concentration occurs across the periphery of the cell membrane resulting in adsorption of solutes. Accordingly, we found that a protein-nanocarrier complex showed high affinity to the membrane after thawing without diffusion into the solution. Moreover, endocytosis was facilitated when combining the freeze-concentration approach with hydrophobic polyampholytes to enhance cytoplasmic internalization due to the high affinity toward the membrane.[15] However, the exact role of the hydrophobic polyampholytes in promoting the internalization of proteins on the cell surface remains poorly understood. Vesicles such as liposomes serve as a useful model for understanding the physicochemical properties of a living cellular system. Cell-sized liposomes are sufficiently large to allow for the real-time observation of transformation and biochemical reactions using optical microscopy.[20] Thus, use of an artificial membrane could be beneficial to understand the physiological properties of a biological system.

In addition, various studies have focused on the use of lipid vesicles that readily undergo a morphological transformation upon external stimulation such as osmotic pressure, shear stress, or temperature that can transform the vesicles into different shapes.[21] This modulation via mechanical forces is generally ascribed as free energy of the membrane, including properties such as curvature and tension.

In the present work, we evaluated the effect of hydrophobic polyampholytes combined with a non-frozen cold temperature on the internalization of gold nanoparticles (AuNPs) into cell-sized liposomes. We adopted a cold temperature rather than the harsh freezing condition reported previously as the external stimulus, since freezing temperature could disrupt the liposome membrane vesicles, whereas this damage is resisted under a moderate cooling condition.[22] In

addition, we chose AuNPs as the model nanomaterials because of their good visualization in microscopy.[23] We further investigated the interaction of hydrophobic polyampholytes and an artificial biomembrane with lateral heterogeneity for modeling a more naturally realistic situation. Together, these results could provide a novel combination for enhancing the internalization of AuNPs to serve in nanomedicine.

2. EXPERIMENTAL SECTION

2.1 Preparation of Hydrophobic Polyampholytes. Self-assembled polyampholyte NPs were prepared according to our prior report.[15] In brief, an aqueous solution of 25% (w/w) ε-PLL of molecular weight about 4000 Da (JNC Co. Ltd., Yokohama, Japan) was hydrophobically modified with a 5% molar ratio of DDSA (Wako Pure Chemical Industries Ltd., Osaka, Japan) at 100°C for 2 h. Thereafter, SA (Wako Pure Chemical Industries Ltd.) was added at a 65% molar ratio to react for 2 h at 50°C. The substitution of SA and DDSA was confirmed by proton nuclear magnetic resonance (^{1}H NMR). ^{1}H NMR spectra were obtained at 25 ˚C on a Bruker AVANCE III 400 spectrometer (Bruker BioSpin Inc., Switzerland) in D_2O.

2.2 Characterization of Hydrophobic Polyampholytes. The surface potential and size of the hydrophobic polyampholytes were characterized using a Dynamic light scattering (DLS) technique (Malvern Instruments, Worcestershire, UK) with a scattering angle of 135° and a temperature of 25°C. The polyampholytes were dispersed in phosphate buffered saline without calcium and magnesium (PBS (-)) and the zeta potential was measured under the default parameters of a dielectric constant at 78.5 and refractive index at 1.6. Data were obtained as an average of more than three measurements on different samples.

2.3 Fluorescent Labeling of Polyampholytes. ε-PLL was labeled with fluorescein isothiocyanate (FITC: λex = 495 nm, λem = 519 nm; Dojindo, Kumamoto, Japan) for confocal

laser-scanning microscopy (CLSM) observations. In brief, an aqueous solution of PLL (25% w/w) was reacted with FITC at a 1/10000 molar ratio for 24 h under constant stirring at room temperature. After completion, the FITC-PLL complex was purified using a dialysis membrane (molecular weight cutoff 3 kDa; Spectra/Por, Spectrum Laboratories, Inc., CA, USA) against water for 48 h, and the dialyzed solution was freeze-dried. The same procedure was used for the preparation of hydrophobically modified polyampholytes using FITC-PLL.

2.4 Preparation of Cell-sized Liposomes. Cell-sized liposomes were prepared by a previously reported hydration method.[24] First, a desired amount of lipids and glucose was dissolved in chloroform in a small glass tube. The organic solvent was evaporated under a nitrogen flow to form a thin film layer of lipids. The glass tubes were then placed in desiccators under vacuum pressure for about 2 h to remove the unevaporated solvent. The film was hydrated with 200 μL Milli-Q water for 3 h. The final concentration of lipids and glucose was 0.2 mM and 0.6 mM, respectively. For fluorescent labeling of the liposomes, N-(rhodamine red-X)-dihexadecanoyl-sn-glycero-phophoethanolamine triethyl ammonium salt (Rh-PE: λex = 560 nm, λem = 580 nm; Invitrogen, Carlsbad, CA, USA) was added at a final concentration of 0.001 mM. The liposomes were composed of either dioleoylphosphatidylcholine (DOPC) alone or a DOPC:dipalmitoylphosphatidylcholine (DPPC):cholesterol (Chol) mixture (40:40:20; Avanti Polar Lipids, Alabaster, AL, USA) for preparation of homogeneous and heterogeneous membranes, respectively.

2.5 Fluorescence Microscopy for Adsorption of Polyampholytes into Liposomes. DOPC liposomes with a total lipid concentration of 0.2 mM (15 μL) were mixed with an aqueous solution of polyampholytes (15 μL). The liposomes and polyampholytes mixture (10 μL) was transferred onto a glass coverslip with a silicone rubber spacer of a thickness of 0.1 mm. The adsorption of

polyampholytes on liposomes was observed using a Biozero 800 microscope system (Keyence, Osaka, Japan).

2.7 Interaction of Polyampholytes and the Laterally Heterogeneous Liposomal Membrane. The interaction of FITC-labeled polyampholytes with the phase-separated surface of the heterogeneous membrane composed of DOPC:DPPC:Chol (40:40:20) was observed using CLSM (CLSM-1000-D; Olympus, Tokyo, Japan).

2.8 Effect of Polyampholytes and Low Temperature on Internalization of AuNPs in Cell-sized Liposomes. DOPC liposomes (15 μL) were mixed with 15 μL of 0.1% (w/v) polyampholytes, and then 30 μL of citrate-capped stabilized AuNPs (50 nm; Sigma Aldrich, St. Louis, MO, USA) was added to the mixture. The solution was transferred to a small microtube, and the temperature of all samples was carefully adjusted to 25°C and −3°C using a freeze-controller program (Cryologic, CL-8800I, Victoria, Australia)

Internalization of the AuNPs with liposomes was then investigated through confocal microscopy. The samples (10 μL) were placed on glass slides including a silicon rubber spacer, and covered with a cover glass for CLSM observation. To obtain scattering images of the 50-nm AuNPs, a laser wavelength of 559 nm with a band pass filter of 535–565 nm was used (Figure S1). For clear observations, z-stacks investigation was acquired from the base to the top of the liposome with a constant step size of 1 μm. The offset and gain of the system were also adjusted to minimize the noise signal during data processing. First, we selected vesicles with a diameter of around 8–10 μm, and the number of sectional images was ≥ 4. The localization of particles (green) inside the aqueous solution (black) surrounded by membranes (red) was observed in more than two images among all of the sectional images of a liposome to determine whether liposome internalization had occurred . The percentage of internalized AuNPs was then calculated with the following equation:

$$\%\ internalization = \frac{Number\ of\ liposomes\ with\ internalization\ of\ AuNPs}{Total\ number\ of\ \ liposomes}$$

3. RESULTS & DISCUSSION

3.1 Synthesis and Characterization of Self-assembled Hydrophobic Polyampholytes. Hydrophobic polyampholytes were successfully prepared by the modification of PLL with DDSA (5 mol%) and SA (65 mol%) as shown in Scheme 1. The successful modification of SA and DDSA was confirmed by ^{1}H NMR (Figure S2).

We denoted the prepared hydrophobic polyampholytes as PLL-DDSA (5)-SA (65), reflecting that the 5% molar ratio of the amino group was converted to DDSA and the 65% molar ratio of the amino group from PLL was substituted with SA. The degree of substitution of DDSA and SA was found to be 3.7% and 66.01%, respectively, as determined by ^{1}H NMR according to the following equations (Figure S3):

Degree of substitution for DDSA (%) = $(2 \times I_{\delta 0.74}/3 \times I_{\delta 1.5\text{-}1.8}) \times 100$

Degree of substitution for SA (%) = $(2 \times I_{\delta 2.4}/4 \times I_{\delta 1.5\text{-}1.8}) \times 100$

Where $I_{\delta 0.74}$ is the integral peak of the methyl group of DDSA located at 0.74 ppm and $I_{\delta 2.4}$ is the integral of the methylene peak of SA located at 2.4 ppm. Moreover, the integral peak of methylene groups in intact PLL was in the range of 1.5–1.8 ppm.

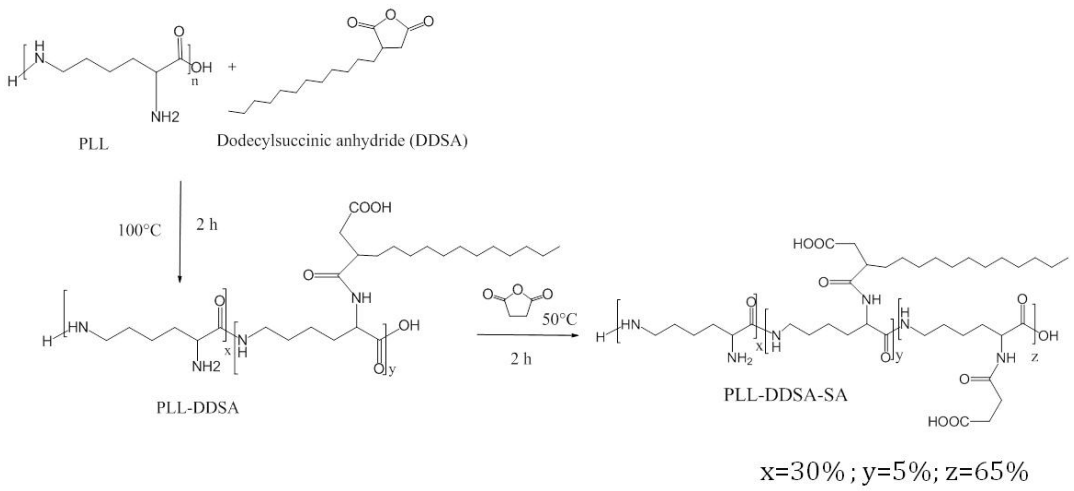

Scheme 1. Synthetic scheme for the generation of hydrophobic polyampholytes (PLL-DDSA-SA)

3.2 Particle Size and Zeta Potential of Polyampholytes. Physicochemical properties such as the particle size and surface potential of nanomaterials show a paramount effect on the interaction of nanomaterials and cell-sized liposomes. Kuhn et al. [25] showed that nanoparticles take on different endocytic paths depending on their particle sizes and other external factors. Therefore, we next investigated the effect of the surface charge and particles size of polyampholytes after modification with SA and DDSA using a dynamic light scattering (DLS) method. The polyampholytes were approximately 17.32 ± 3.58 nm in diameter at pH 7.4 in line with our previous report (Figure S4 (A)).[15] Akiyoshi et al.[26,27] reported the self-aggregation of hydrophobic polysaccharides in an aqueous medium through inter/intramolecular associations, with a diameter that was also around 30 nm. Thus, this same self-aggregation phenomenon observed in hydrophobic polyampholytes with significantly nano-sized particles after random modification by hydrophobic DDSA and SA is likely due to the intermolecular hydrophobic and electrostatic interactions that result in compact packing of hydrophobic groups. This hypothesis was confirmed by estimation of the critical aggregation concentration of the polyampholytes, which was found to

be very low (around 0.1 mg/mL) in our previous study,[15] resulting in more ready aggregation through intermolecular hydrophobic interaction.

The zeta potential of the hydrophobic polyampholytes shifted toward a negative value of −15.91 mV after modifying the amino to carboxyl group. However, the surface potential of native PLL was 17.11 mV (Figure S4 (B)). These results indicated that the modification of carboxyl groups such as DDSA and SA was successfully carried out in PLL. Various reports have demonstrated that cationically charged materials have toxicity under certain concentrations. However, these negatively charged hydrophobic polyampholytes were shown to be efficient nanocarriers for protein delivery with low toxicity in our previous study.[15]

3.3 Hydrophobic Polyampholytes Adsorbed on DOPC Liposomes. The association of polyampholytes and cell-sized DOPC liposomes was evaluated with optical microscopy. The polyampholytes were labeled with fluorescent FITC dye while the DOPC liposomes were conjugated with the fluorescent lipid Rh-PE. The polyampholyte solution was prepared in Milli-Q water at pH 7.4 at different concentrations from 0.05% to 0.6% (w/v). Figure 1 (A–E) displays the association of the FITC-labeled polyampholytes onto the liposome membrane. We observed a gradual increase in the adsorption of polyampholytes towards the DOPC liposome membrane with an increase in the polyampholyte concentration, indicating that the polyampholytes preferentially show an adhesive property toward the liposome membrane. The adsorption of polyampholytes onto liposomes might be attributed to the hydrophobic groups, specifically the hydrocarbon chains, of polyampholytes (Figure 1 A–E). However, with an increasing concentration of polyampholytes at 0.6% (w/v), the membrane bilayer became destabilized, which was possibly due to aggregation of polyampholytes particles particularly around the membrane (Figure 1E). Therefore, for further experiments, we chose 0.1% (w/v) as the optimized concentration of hydrophobic polyampholytes

to elucidate the physicochemical interaction between liposome membranes and polyampholytes. Overall, this outcome suggests the excellent ability of hydrophobic polyampholytes to adsorb phospholipids and their high affinity toward cell-sized liposomes.

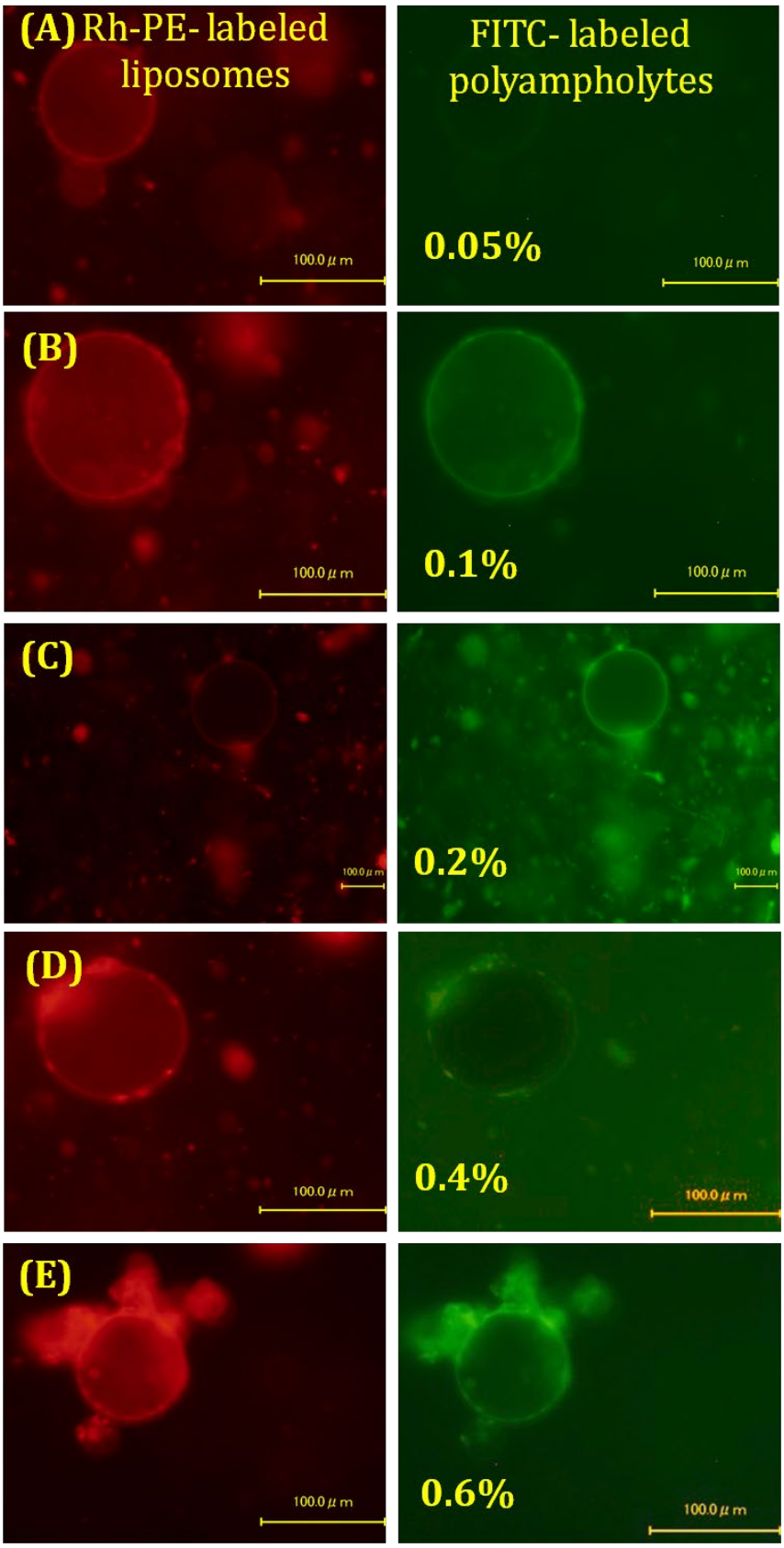
(A) Rh-PE- labeled liposomes
FITC- labeled polyampholytes
0.05%
100.0 μm
(B)
0.1%
(C)
0.2%
(D)
0.4%
(E)
0.6%

Figure 1 Fluorescent images of Rh-PE-labeled DOPC liposomes and FITC-labeled polyampholytes. (A–E) Adsorption of FITC-labeled hydrophobic polyampholytes at a concentration of 0.05% to 0.6% (w/v), respectively, and Rh-PE labeled DOPC liposomes using a fluorescent microscope. Scale bar: 100 μm.

3.4 Interaction of Hydrophobic Polyampholytes with Laterally Heterogeneous Membranes. The plasma membrane typically forms micro-domains called rafts, which show a lateral organization with a higher lipid order that is rich in cholesterol and saturated lipids.[28,29] This raft is considered to be in the form of order- and disorder-phase separation due to the interactions between membrane lipids. The great advantage of using a "raft"-based lipid membrane system is the similar bilayer structure to natural membranes for exploring various applications such as in signal transduction[30], cell adhesion[31], and vesicle trafficking[32], as essential processes for cellular movement or division. A previous report demonstrated the ability to visualize the phase separation behavior of the lipid bilayer using cell-sized liposomes. In fact, the membrane phase is divided into three states based on the lipid composition: liquid-disorder (Ld), liquid-order (Lo), and solid-order (So).[33] In particular, the existence of two liquids between the Lo and Ld states has received substantial research attention because of the strong correlation of the Lo phase to lipid rafts of the physiological membrane.[34-38] In our previous investigation, we observed the efficacy of hydrophobic polyampholytes only on DOPC liposomes alone. Therefore, it is crucial to further explore the interaction of polyampholytes with a more natural heterogeneous membrane interface. Toward this end, we used saturated and unsaturated lipids as DPPC, and DOPC and Chol to observe the interaction of hydrophobic polyampholytes with two liquid phase-separated liposomes, Lo-phase (DPPC and Chol-rich) and Ld-phase (DOPC rich). The liposomal membrane was conjugated with the red fluorescent lipid Rh-PE, which preferably belongs to the Ld phase, and

FITC-labeled polyampholytes were mixed with the phase-separated liposomes DOPC:DPPC:Chol (40:40:20). Interestingly, examination of the localization of hydrophobic polyampholytes on the phase-separated membrane surface showed the selective distribution of polyampholytes in the Ld rather than in the Lo phase based on both cross-section as well as surface images Figure 2. Previously, we found that smaller particles tended to localize in the ordered phase while larger particles were more frequently observed in the Ld phase.[27] In another study, the interaction between Amyloid beta (Aβ) peptides and liposomes have been studied. This peptide consists of 40-42 amino acid residues, responsible in the death of neural cells in Alzheimer's diseases.[38,39] Aβ-42 was found to be selectively localized in the Ld region after a change in the motion of Lo domains.[38] However, in the present study, the hydrophobic polyampholytes were selectively distributed in the disordered phase rather than in the ordered phase. Nanomaterials have a tendency to show selective localization in phase-separated liposomes consisting of well-organized domains. Since the hydrophobic polyampholytes on a bilayer membrane selectively showed partition in the disordered phase, in subsequent experiments we focused on DOPC liposomes instead of phase-separated liposomes as the hydrophobic polyampholytes showed greater affinity toward the DOPC lateral compartments.

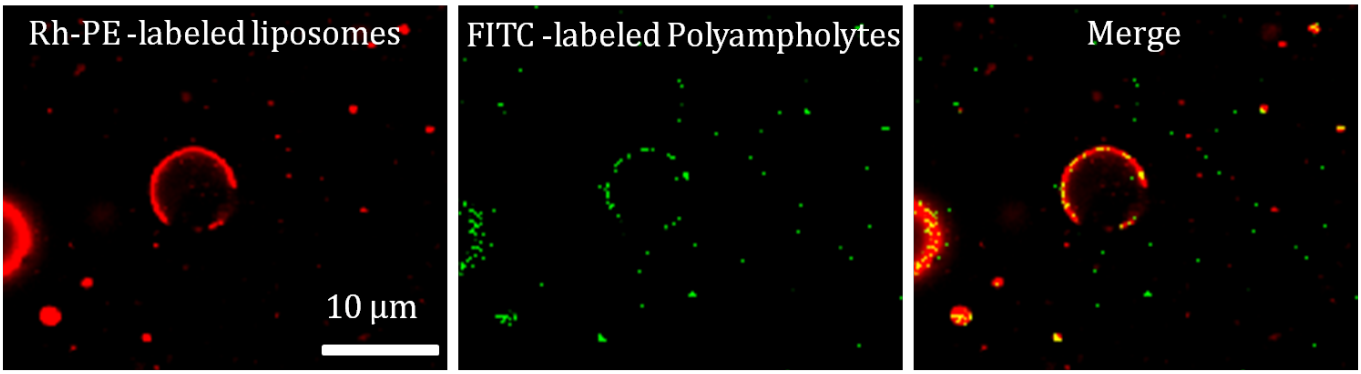

Figure 2 In-section confocal images of the localization of polyampholytes on cell-sized liposomes. Polyampholytes were incubated with liposomes consisting of DOPC: DPPC: Chol (40:40:20),

showing the existence of Lo/Ld phases. The red and green fluorescence is from Rh-PE and FITC, respectively. Scale bar: 10 μm.

3.5 Influence of Temperature and Hydrophobic Polyampholytes on AuNP Internalization into Cell-sized Liposomes. The transportation of particles into cells is of great interest for nanomedicine applications. In general, when particles approach a membrane, the membrane becomes susceptible to a structural transformation such as budding, fission, and pore formation.[40,41] Such deformations of the membrane are induced by various chemical stimuli such as peptides and surfactants.[42] In addition, physical stimuli such as light[43] as well as osmotic pressure[44] have also been shown to deform the membrane. In this study, we combined both chemical (hydrophobic polyampholytes) and physical (cold temperature) stimuli to induce the internalization of nanomaterials.

We first observed the liposomes at 25°C as well as in the cold temperature of −3°C with incubation of 5, 30, and 60 min using a freeze-controller instrument. The penetration of AuNPs was examined under the two temperature conditions for 60 min with or without hydrophobic polyampholytes using z-stack analysis through confocal microscopy (Figure 3 A–D). The sectional images showed that the AuNPs did not surround the liposomes even after long-term incubation at 25°C (Figure 3A), whereas under cold temperature (−3°C), more of the AuNPs had penetrated the liposomes after a longer incubation time (Figure 3B). However, when hydrophobic polyampholytes were mixed with AuNPs at 25°C, the strong presence of AuNPs inside the aqueous solution of liposomes vesicles was observed (Figure 3C). The entry of nanoparticles was further enhanced by the incorporation of polyampholytes along with low temperature (Figure 3D). The graph of internalized AuNPs over time from selected sectional images of at least four liposomes

in each condition demonstrated a clear association between hydrophobic polyampholytes and cold temperature to promote the entry of AuNP in the vesicles. Interestingly, the diffusion of AuNPs inside liposomes was most strongly promoted at −3°C with hydrophobic polyampholytes compared to all other conditions tested (Figure 3E)

(A) At 25 ˚C without hydrophobic polyampholytes

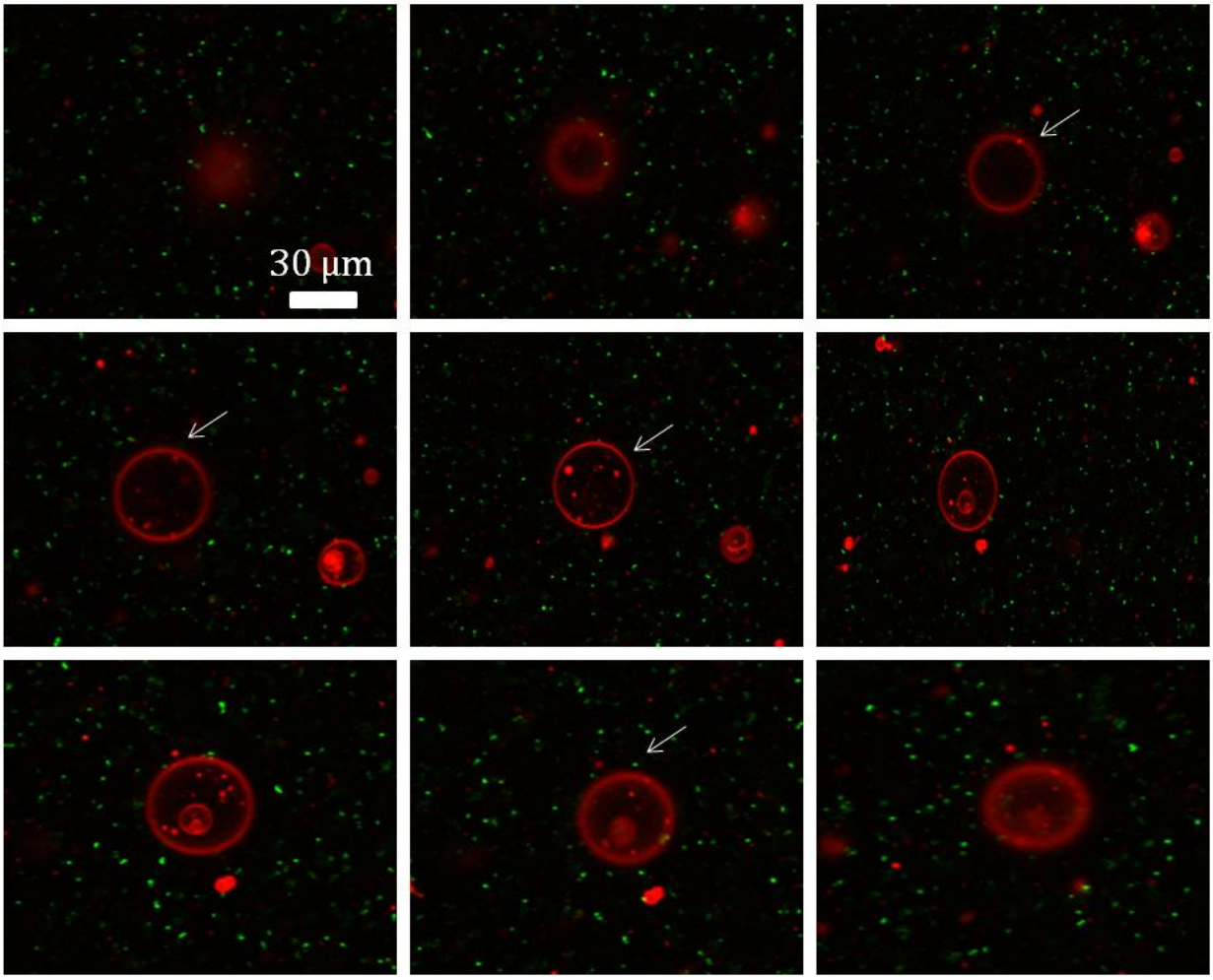

(B) At -3 ˚C without hydrophobic polyampholytes

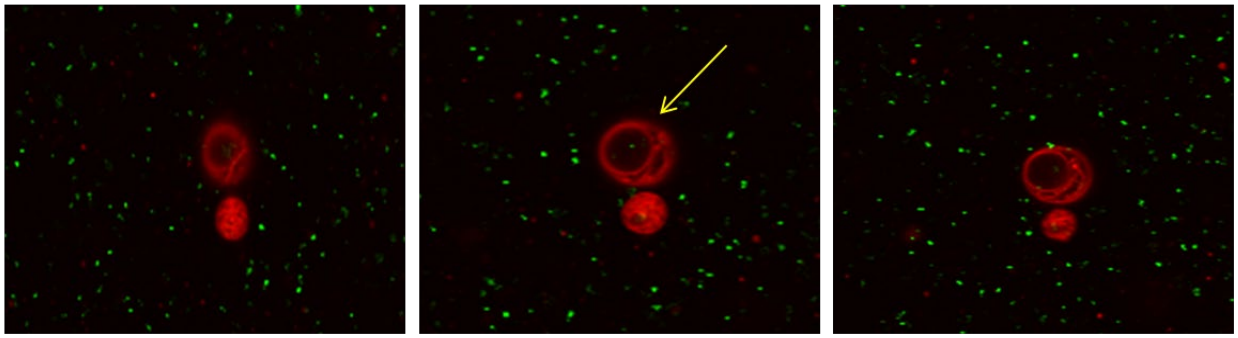

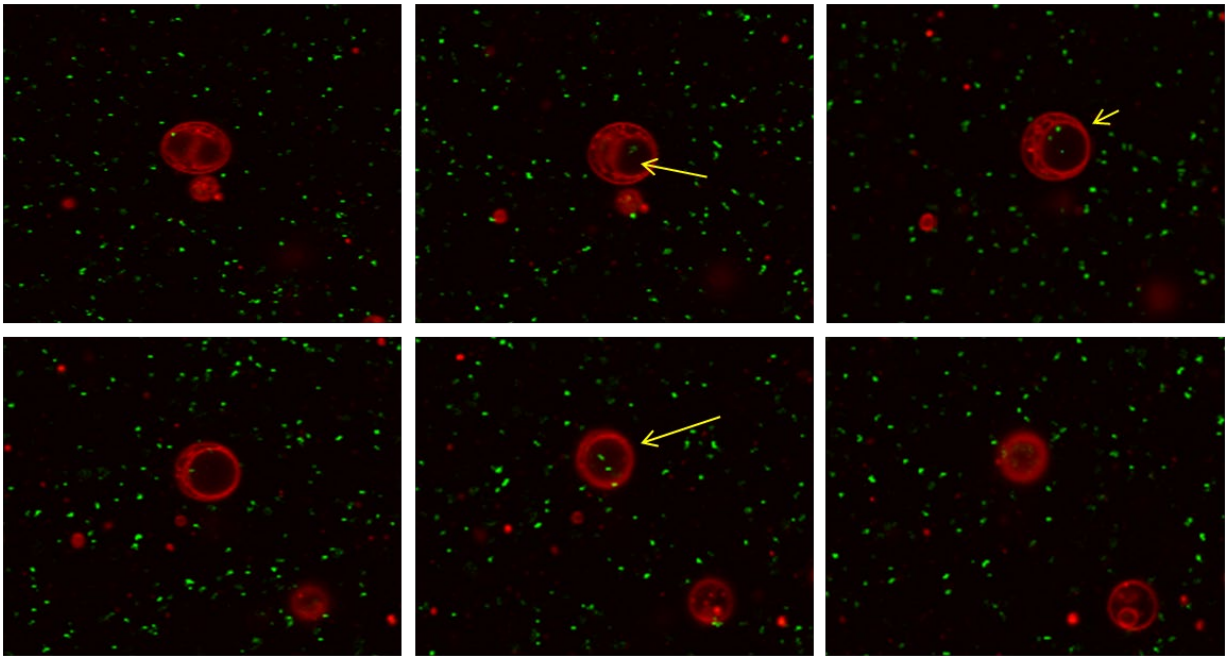

(C) At 25°C with hydrophobic polyampholytes

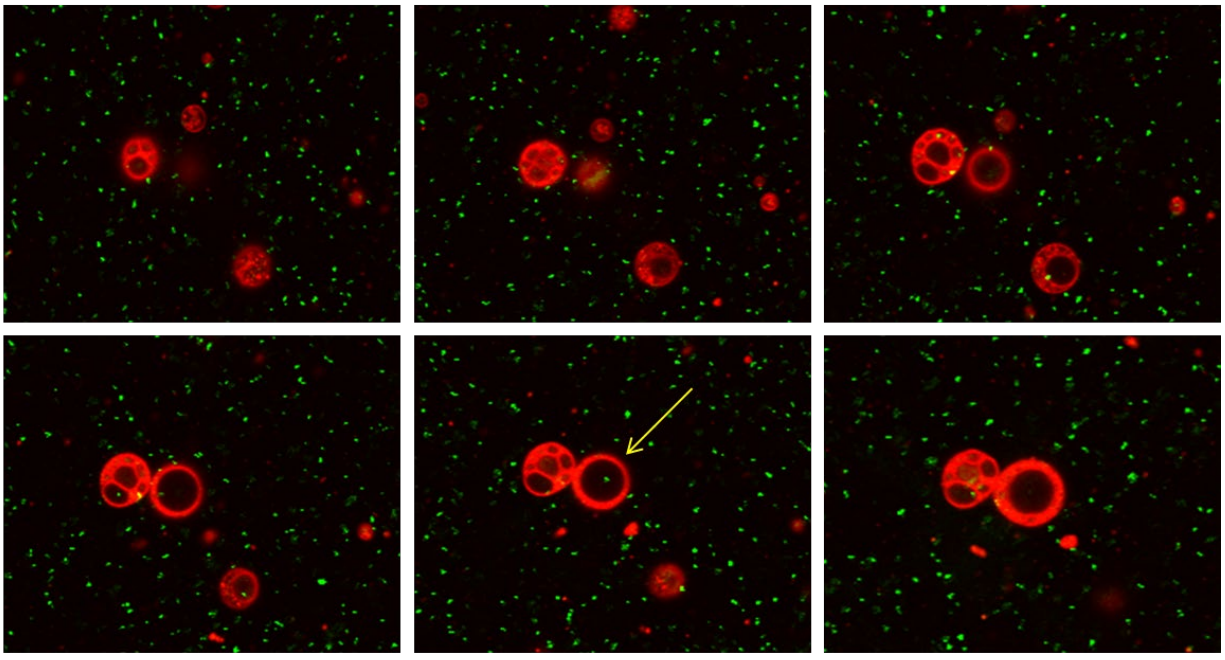

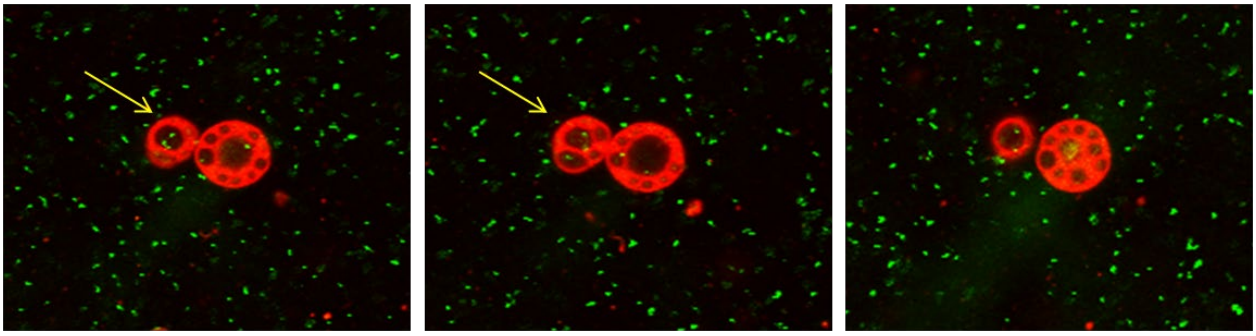

(D) At -3 °C with hydrophobic polyampholytes

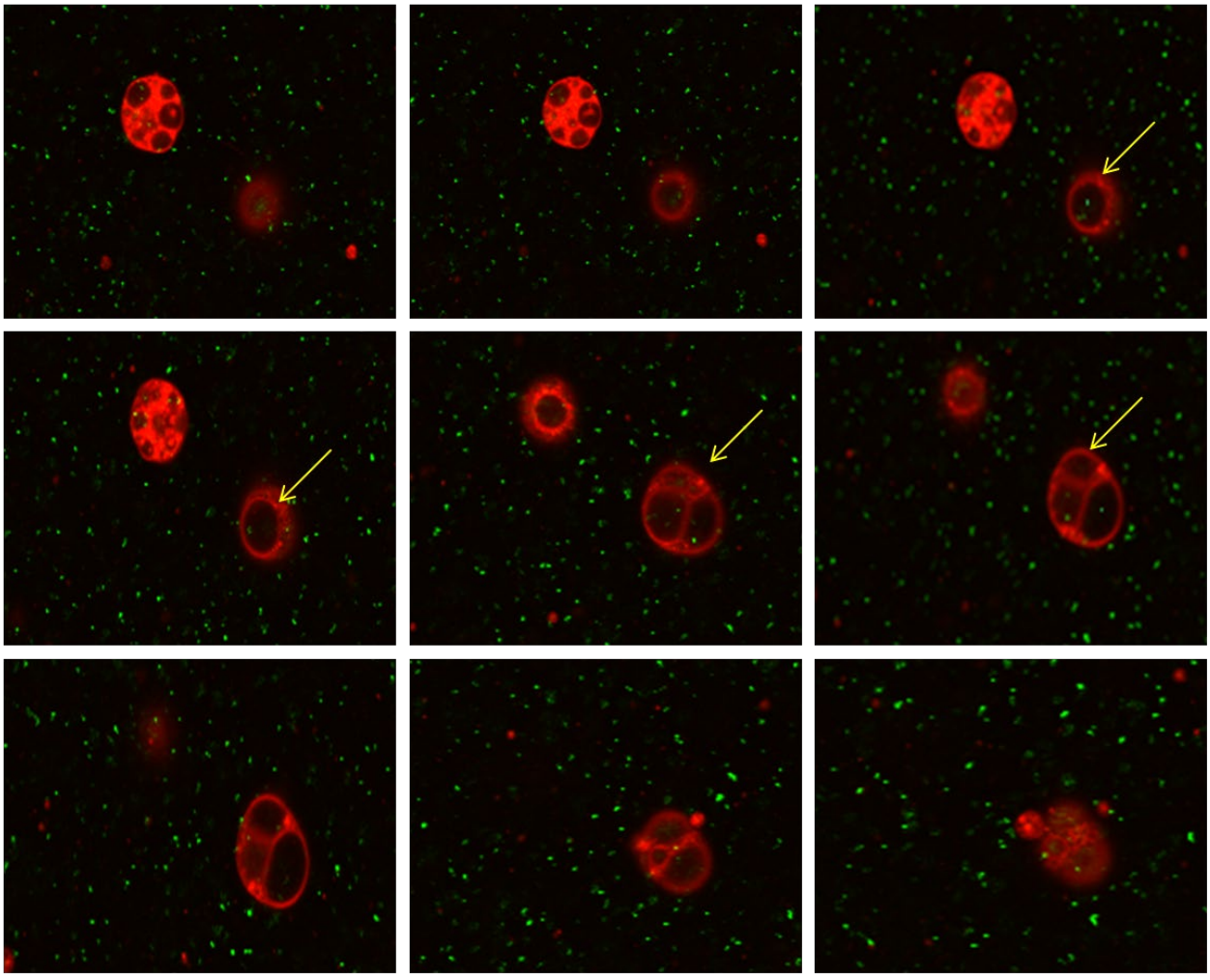

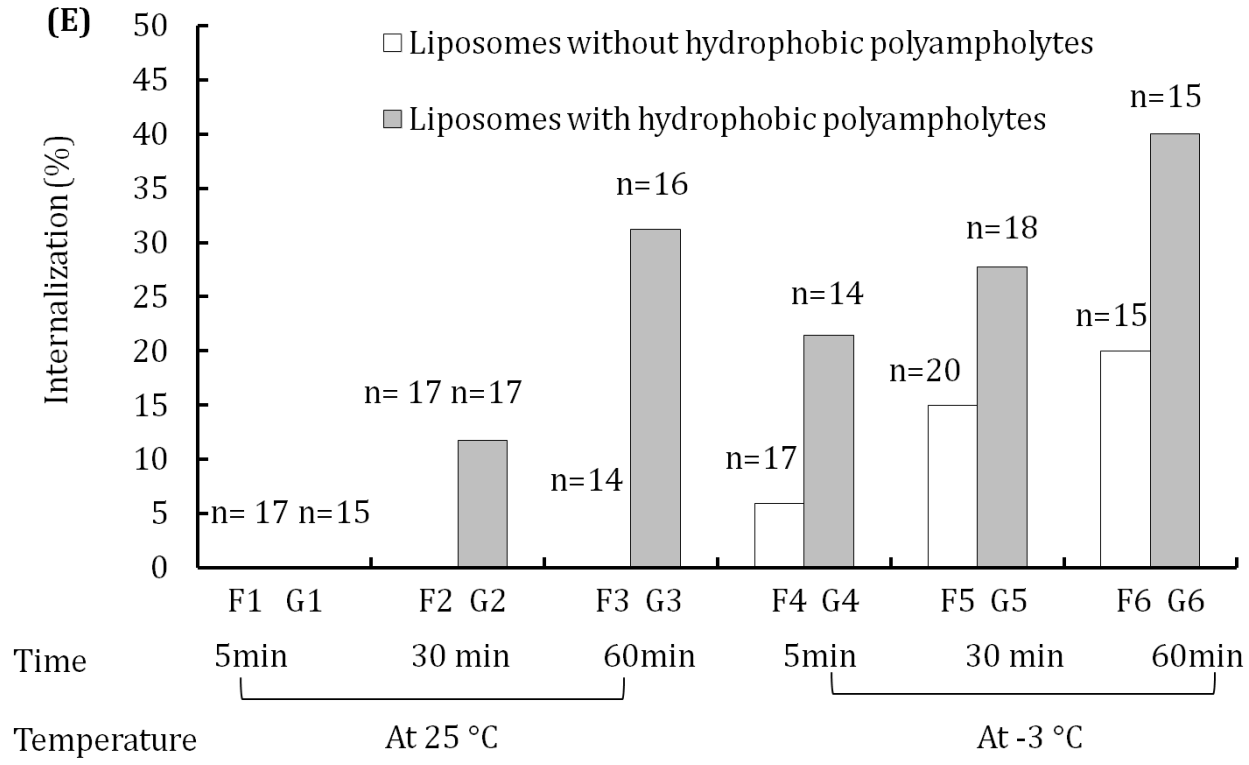

Figure 3 Confocal top-to-bottom z-stack merge images of scattered AuNPs into Rh-PE-labeled DOPC liposomes (starting from the left to right panel) in the presence or absence of polyampholytes after incubating for 60 min at two different temperatures: 25°C and –3°C. (A) Without polyampholytes at 25°C. (B) Without polyampholytes at –3°C. (C) With polyampholytes at 25°C. (D) With polyampholytes at –3°C. At least four sectional images were analyzed for each condition. The localization of particles (green) inside the aqueous solution (black) surrounded by membranes (red) for more than two images among all sectional images of a liposome was considered to indicate the internalization of AuNPs into cell-sized liposomes. The white arrow indicates lack of internalization and the yellow arrow indicates internalization. Scale bar: 30 μm. (E) Plot of the percent internalization of AuNPs at 25°C and –3°C for different incubation times

(5, 30, and 60 min). F, liposomes without hydrophobic polyampholytes; G, liposomes with hydrophobic polyampholytes; 1–3, incubation for 5, 30, and 60 min at 25°C, respectively; 4–6, incubation for 5, 30, and 60 min at –3°C, respectively. The number of sectional liposomes vesicles (n) selected for each condition is indicated above the bars.

Although the precise mechanism by which hydrophobic polyampholytes induce the penetration of AuNPs is not completely clear, one possibility is that the hydrophobic polyampholytes may localize at the edge of the liposomal bilayer due to their amphiphilic property, resulting in a certain degree of pore stabilization.[45] Protein also leads to show vesicle pore formation.[46] Consequently, when the temperature decreases, the surface area of the liposomes would also decrease so as to increase the inner pressure in the system and raise the membrane tension, thereby generating a pore to release the pressure.[47] These effects could lead to the formation of transient pores, which may induce the transportation of AuNPs into the cell-sized vesicles.

Although this mechanism and other possibilities should be further tested with detailed experiments, our findings clearly demonstrate that the combination of low temperature and hydrophobic polyampholytes can effectively induce the internalization of AuNPs in cell-sized liposomes, providing a baseline strategy for improving nanomedicine.

CONCLUSIONS

We used cell-sized liposomes for the delivery of nanoparticles combined with hydrophobic polyampholytes and cold stress. The hydrophobic polyampholytes tended to localize on disordered membranes rich in unsaturated DOPC lipids. Moreover, the addition of hydrophobic polyampholytes enhanced the penetration of AuNPs with the aid of low temperature. These results

point to the efficacy of hydrophobic polyampholytes for increasing the endocytic pathways to promote the nanomaterials-based delivery of therapeutics. Overall, we expect that use of an artificial membrane can further help to gain a fundamental understanding of the delivery system process, representing a promising approach in nanomedicine.

ASSOCIATED CONTENT

Supporting Information

Supporting Information is available free of charge on the ACS Publications website at DOI:

Schematic description of the setting of confocal microscopy observations; ^{1}H NMR of native PLL and PLL-DDSA-SA; integration of ^{1}H NMR of PLL-DDSA(5)-SA(65); zeta potential of PLL and PLL-DDSA-SA. (PDF)

AUTHOR INFORMATION

Corresponding Authors

*Tsutomu Hamada, e-mail: t-hamada@jaist.ac.jp; Tel: +81-761-51-1670; Fax: +81-761-51-1672

*Kazuaki Matsumura, e-mail: mkazuaki@jaist.ac.jp; Tel: +81-761-51-1680; Fax: +81-761-51-1149. ORCID: 0000-0001-9484-3073

Funding Sources

This study was supported in part by Japan Society for the Promotion of Science (JSPS), KAKENHI Grants [16K12895 (KM), 17H02942 (TH), and 15K12538 (TH)], and Japan Agency for Medical Research and Development (AMED) under Grant Number JP17gm0810006 (TH).

Notes

The authors declare no competing financial interest.

REFERENCES

1. Lakshmanan, S.; Gupta, G.K.; Avci, P.; Chandran, R.; Sadasivam, M.; Jorge, A.E.; Hamblin, M.R. Physical energy for drug delivery; poration, concentration and activation. *Adv Drug Deliv. Rev.* **2014**, *71*, 98-114.

2. Singh, V.K.; Behera, B.; Pramanik, K.; Pal, K. Ultrasonication-assisted preparation and characterization of emulsion and emulsion gels for topical drug delivery. *J Pharm Sci.* **2015**, *104* (3), 1035-1044.

3. Munyendo, W.L.L.; Huixia, L.; Benza-Ingoula, H.; Baraza, L.D.; Zhou, J. Cell penetrating peptides in the delivery of biopharmaceuticals. *Biomolecules* **2012**, *2*, 187-202.

4. Martins, S.; Sarmento, B.; Ferreira, D.C.; Souto, E.B. Lipid-based colloidal carriers for peptide and protein delivery-liposome versus lipid nanoparticles. *Int J Nanomedicine* **2007**, *2* (4), 595-607.

5. Jiang, Y.; Lu, H.; Chen, F.; Callari, M.; Pourgholami, M.; Morris, D.L.; Stenzel, M.H. PEGylated Albumin-based polyion complex Micelles for protein delivery. *Biomacromolecules* **2016**, *17* (3), 808-817.

6. Nochi, T.; Yuki, Y.; Takahashi, H.; Sawada, S.; Meijima, M.; Kohda, T.; Harada, N.; Kong, G.; Sato, A.; Kataoka, N.; Tokuhara, D.; Kurokawa, S.; Takahashi, Y.; Tsukada, H.; Kozaki,

S.; Akiyoshi, K.; Kiyono, H. Nanogel antigenic protein-delivery system for adjuvant-free intranasal vaccines. *Nat. Mater.* **2010**, *9*, 572-578.

7. Pan, Y.; Li, Y.J.; Zhao, H.Y.; Zheng, J.M.; Xu, H.; Wei, G.; Hao, J.S.; Cui, F.D. Bioadhesive polysaccharide in protein delivery system: chitosan nanoparticles improve the intestinal absorption of insulin in vivo. *Int J Pharm* **2002**, *249*, 139-147.

8. Solaro, R.; Chiellini, F.; Battisti, A. Targeted delivery of protein drugs by nanocarriers. *Materials* **2010**, *3*, 1928-1980.

9. Kafil, V.; Omidi, Y.; Cytotoxic impacts of linear and branched polyethyleneimine nanostructures in A431 cells. *Bioimpacts* **2011**, *1*(1), 23-30.

10. Wang, Q.; Shen, M.; Zhao, T.; Xu, Y. ; lin, J.; Duan, Y.; Gu, H. Low toxicity and long circulation time of polyampholyte-coated magnetic nanoparticles for blood pool contrast agents. *Sci. Rep.* **2015**, *5*, 7774- 7782.

11. Matsumura, K.; Hyon, S.H.; Polyampholytes as low toxic efficient cryoprotective agents with antifreeze protein properties. *Biomaterials* **2009**, *30*, 4842-49.

12. Gunkel, G.; Weinhart, M.; Becherer, T.; Haag, R.; Huck, W.T.S. Effect of polymer brush architecture on antibiofouling properties. *Biomacromolecules* **2011**, *12*, 4169-72.

13. Zurick, K.M.; Bernards, M. Recent biomedical advances with polyampholyte polymers. *J. Appl. Polym. Sci.* **2014**, *131*, 1-9.

14. Shen, H.; Akagi, T.; Akashi, M. Polyampholyte nanoparticles prepared by self-complexation of cationized poly (γ-glutamic acid). *Macromol. Biosci.***2012**, *12*, 1100-1105.

15. Ahmed, S.; Hayashi, F.; Nagashima, T.; Matsumura, K. Protein cytoplasmic delivery using polyampholyte nanoparticles and freeze concentration. *Biomaterials* **2014**, *35*, 6508-6518.

16. Ahmed, S.; Fujita, S.; Matsumura, K.; Enhanced protein internalization and efficient endosomal escape using polyampholyte-modified liposome and freeze concentration. *Nanoscale* **2016**, *8*, 15888-15901.

17. Ahmed, S.; Fujita, S.; Matsumura, K.; A freeze-concentration and polyampholyte-modified liposomes-based antigen-delivery system for effective immunotherapy. *Adv. Healthc. Mater.* **2017**, *6*, 1-12.

18. Ahmed, S.; Hirabayashi, T.N.; Watanabe, T.; Hohsaka, T.; Matsumura, K.; Freezing-assisted gene delivery combined with polyampholyte nanocarriers. *ACS Biomater. Sci. Eng.* **2017**, *3* (8), 1677-1689.

19. Ahmed, S.; Miyawaki, O.; Matsumura, K.; Enhanced Adsorption of a Protein-Nanocarrier complex onto Cell Membranes through High Freeze Concentration by a Polyampholyte Cryoprotectant. *Langmuir* **2018**, *34*(6), 2352-2362.

20. Hamada, T., Yoshikawa, K., Cell-sized liposome and droplets: Real-world modeling of living cells. *Materials***2012**, *5*, 2292-2305.

21. Tsuda, S., Sakakura, T., Fujii, S., Suzuki, H., Yomo, T., Shape Transformation of Lipid vesicles by insertion of bulky-head lipids. *PLoS ONE* **2015**, *10* (7), 1-16.

22. Kobayashi, M.; Nemoto, K.; Tanaka G.; Hishida, M.; Study of the freezing behavior of liposomes. *J Therm Sci Tech-Jpn* **2011**, *6*, 57-68.

23. Klein, S.; Petersen, S.; Taylor, U.; Rath, D.; Barcikowski, S., Quantitative visualization of colloidal and intracellular gold nanoparticles by confocal microscopy. Monolayer coated gold nanoparticles for delivery applications. *J Biomed Opt.* **2010**, *15*(3), 1-11.

24. Tsumoto, K.; Motsuo, H.; Tomita, M.; Yoshimura, T. Efficient formation of giant liposomes through the gentle hydration of phosphatidylcholine films doped with sugar. *Colloids Surf B Biointerface* **2009**, *68*(1), 98-105.

25. Kuhn, D.A., Vanhecke, D., Michen, B., Blank, F., Gehr, P., Petri-Fink, A., Rutishauser, B.R. Different endocytic uptake mechanism for nanoparticles in epithelial cells and macrophages. *Beilstein J Nanotechnol.* **2014**, *5*, 1625-1636.

26. Morimoto, N., Hirano, S., Takahashi, H., Leothen, S., Thompson, D.H., Akiyoshi, K., Self-assembled pH-sensitive cholesteryl pullulan nanogel as a protein delivery vehicle. *Biomacromolecules***2013**, *14*, 56-63.

27. Akiyoshi, K., Kobayashi, S., Shichibe, S., Mix, D.; Baudys, M., Wan Kim, S., Sunamoto, J., Self-assembled hydrogel nanoparticles of cholesterol-bearing pullulan as a carrier of protein drugs: complexation and stabilization of insulin. *J. Control Release* **1998**, *54*, 313-320.

28. Hamada, T., Morita, M., Miyakawa, M., Sugimoto, R., Hatanaka, A., Vestergaard, M.C., Takagi, M., Size-dependent partitioning of nano/microparticles mediated by membrane lateral heterogeneity. *J. Am. Chem. Soc.* **2012**, *134*, 13990-13996.

29. Sengupta, P., Baird, B., Holowka, D. Lipid Rafts, fluid/fluid phase separation, and their relevance to plasma membrane structure and function. *Semin. Cell Dev Biol.* **2007**, *18* (5), 583-590.

30. Kabouridis, P.S., Lipid rafts in T cell receptor signaling. *Mol Membr Biol*. **2006**, *23*, 49-57.

31. Manes, S., Viola, A. Lipid rafts in lymphocyte activation and migration. *Mol Membr Biol.* **2006**, *23*, 59-69.

32. Parton, R.G., Richards, A.A. Lipid rafts and caveolae as portals for endocytosis: new insights and common mechanism. *Traffic* **2003**, *4* (11), 724-738.

33. Heberle, F.A.; Feigenson, G.W.; Phase separation in lipid membranes. *Cold Spring Herb Perspect. Biol.* **2011**, *3*(4), 1-13.

34. Morita, M.; Hamada, T.; Vestergaard, M.C.; Takagi, M. Endo- and Exocytic budding transformation of slow-diffusing membrane domains induced by Alzheimer's Amyloid Beta. *Phys. Chem. Chem. Phys*., **2014**, *16*, 8773-8777.

35. Dietrich, C.; Bagatolli, I.A.; Volovyk, Z.N.; Thompson, N.; Levi, M.; Jacobson, K.; Gratton, E. Lipid rafts reconstituted in model membranes. *Biophys. J.* **2001**, *80*, 1417-1428.

36. Feigenson, G.W.; Phase diagram and lipid domains in multicomponent lipid bilayer mixtures. *Biochim. Biophys. Acta* **2009**, *1788*, 47-52.

37. Veatch, S.L.; Keller, S.L. Separation of liquid phases in giant vesicles of ternary mixtures of phospholipids and cholesterol. *Biophys. J.* **2003**, *85*, 3074-3083.

38. Morita, M.; Hamada, T.; Tendo, Y.; Hata, T.; Vestergaard, M.C.; Takagi, M. Selective localization of Alzheimer's amyloid beta in membrane lateral compartment. *Soft Matter* **2012**, *8*, 2816-2819.

39. Hardy, J.; Selkoe, D.J. The amyloid hypothesis of Alzheimer's disease: progress and problems on the road to therapeutics. *Science* **2002**, *297*, 353-356.

40. Marrink,S.J.; de Vries, A.H.; Tieleman, D.P. Lipids on the move: Simulations of membrane pores, domains, stalks and curves. *Biochim Biophys Acta* **2009***, 1788,* 149-168.

41. Ishii, K.I.; Hamada, T.; Hatakeyama, M.; Sugimoto, R.; Nagasaki, T.; Takagi, M. Reversible control of exo-and endo-budding transitions in a photosensitive lipid membrane. *Chem Bio Chem* **2009**, *10*, 251-256.

42. Hamada, T.; Hagihara, H.; Morita, M.; Vestergaard, M.C.; Tsujino, Y.; Takagi, M. Physicochemical profiling of surfactant-induced membrane dynamics in a cell-sized liposome. *J. Phys. Chem. Lett.* **2012**, *3*,430-435.

43. Suzuki, Y.; Nagai, K.H.; Zinchenko, A.; Hamada, T. Photo-induced fusion of lipid bilayer membranes. *Langmuir* **2017**, *33*, 2671-2676.

44. Ohno, M.; Hamada, T.; Takiguchi, K.; Homma, M. Dynamic behavior of giant liposomes at desired osmotic pressure. *Langmuir* **2009**, *25*(9), 11680-11685.

45. Hamada, T.; Hirabayashi, Y.; Ohta, T.; Takagi, M. Rhythmic pore dynamics in a shrinking lipid vesicles. Phys. Rev. E., **2009**, *80*, 1-7.

46. Saitoh, A.; Takiguchi, K.; Tanaka, Y.; Hotani, H., Opening-up of liposomal membranes by talin. *Proc. Natl. Acad. Sci. USA* **1998**, *95*, 1026-1031.

47. Sakuma, Y.; Taniguchi, T.; Imai, M. Pore formation in a binary giant vesicle induced by cone-shaped lipids. *Biophys. J.* **2010**, *99*, 472-479.

Table of Content figure

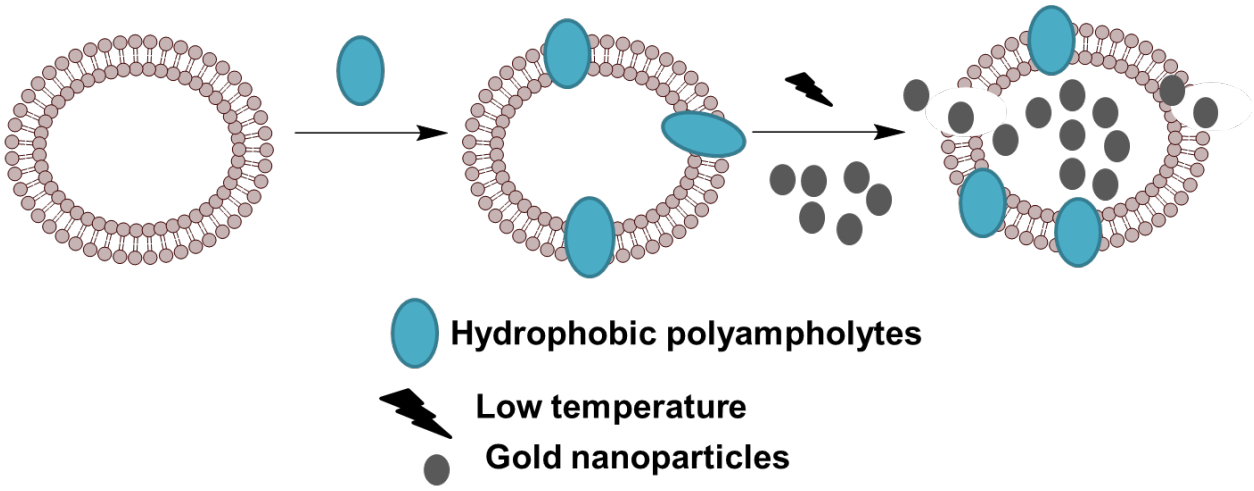

Supporting Information for

Hydrophobic Polyampholytes and Nonfreezing Cold Temperature Stimulate Internalization of Au Nanoparticles to Zwitterionic Liposomes

Sana Ahmed, Kazuaki Matsumura[*] and Tsutomu Hamada[*]

[*]Corresponding authors

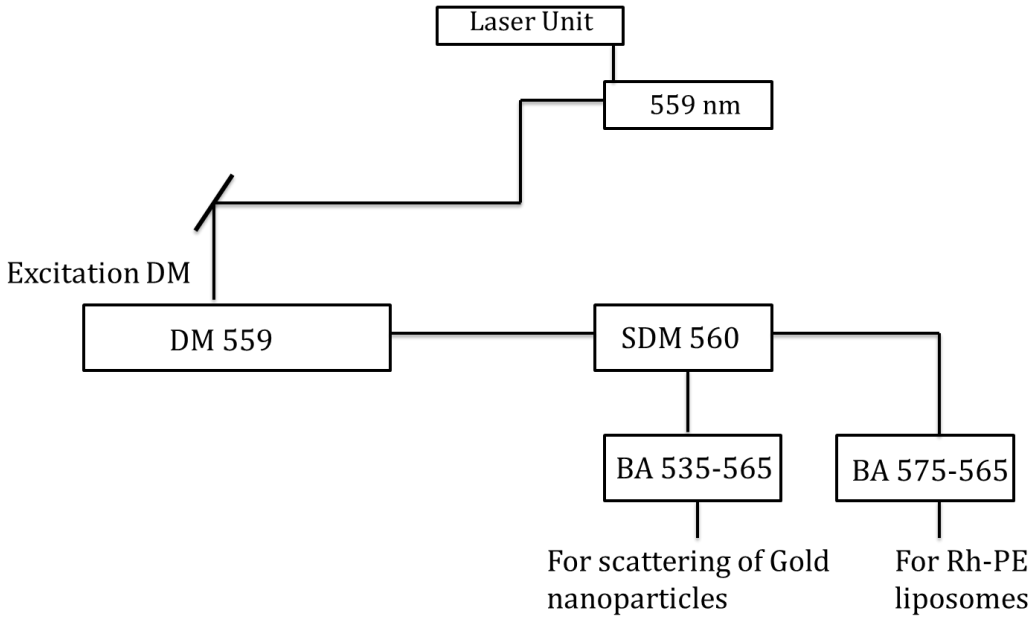

Figure S1 Schematic description of the setting of confocal microscopy for observation of the scattering of AuNPs along with Rh-PE liposomes

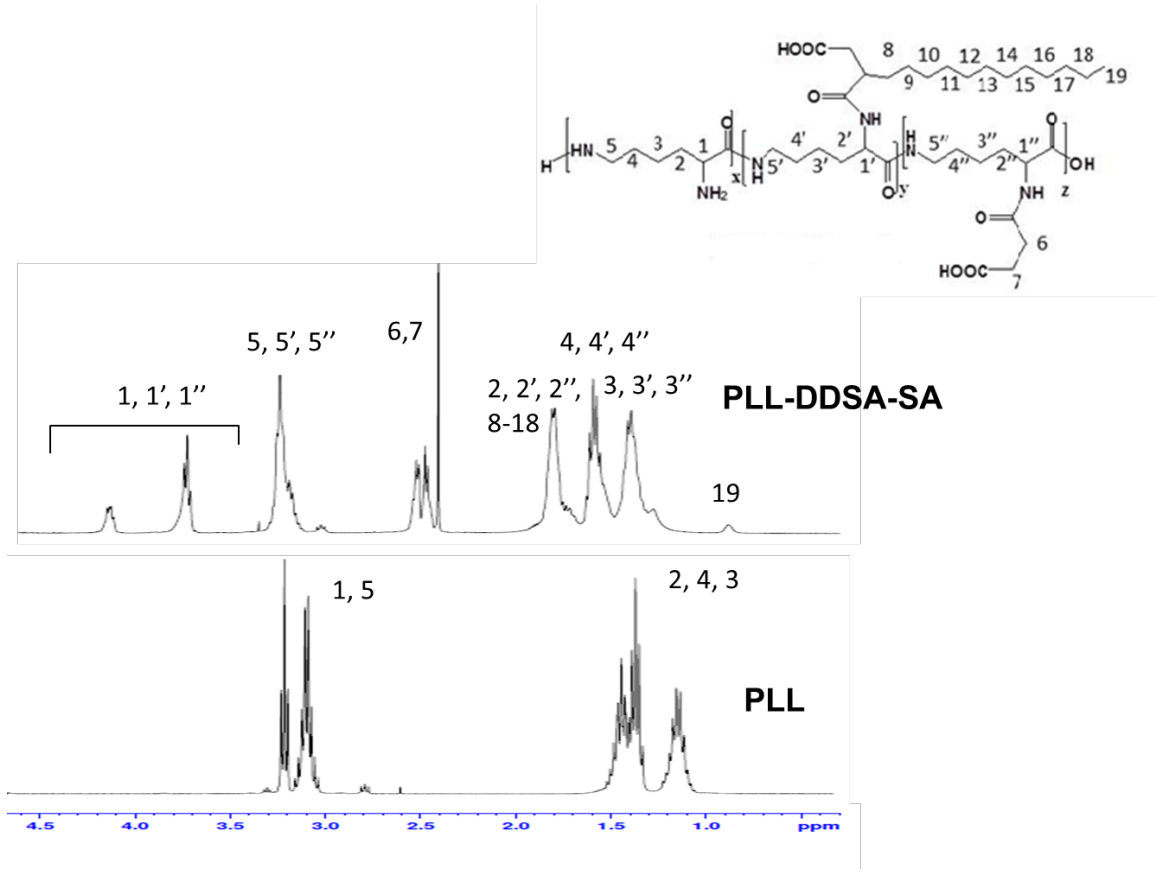

Figure S2 ^{1}H NMR of native PLL and PLL-DDSA-SA

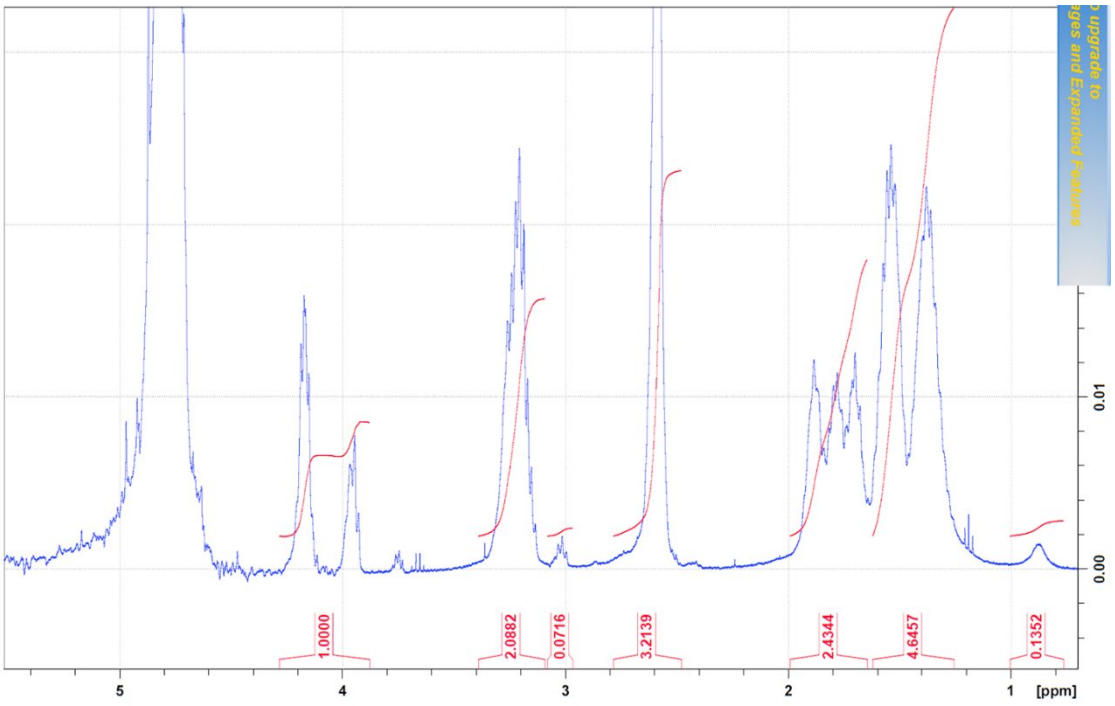

Figure S3 Integration of ^{1}H NMR of PLL-DDSA(5)-SA(65)

(A)

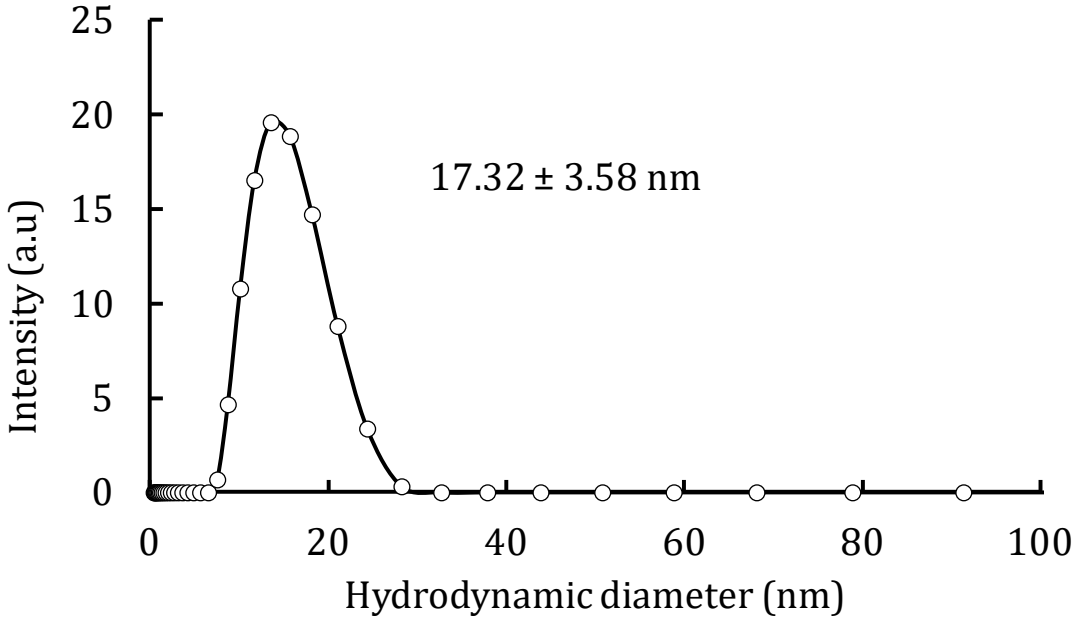

(B)

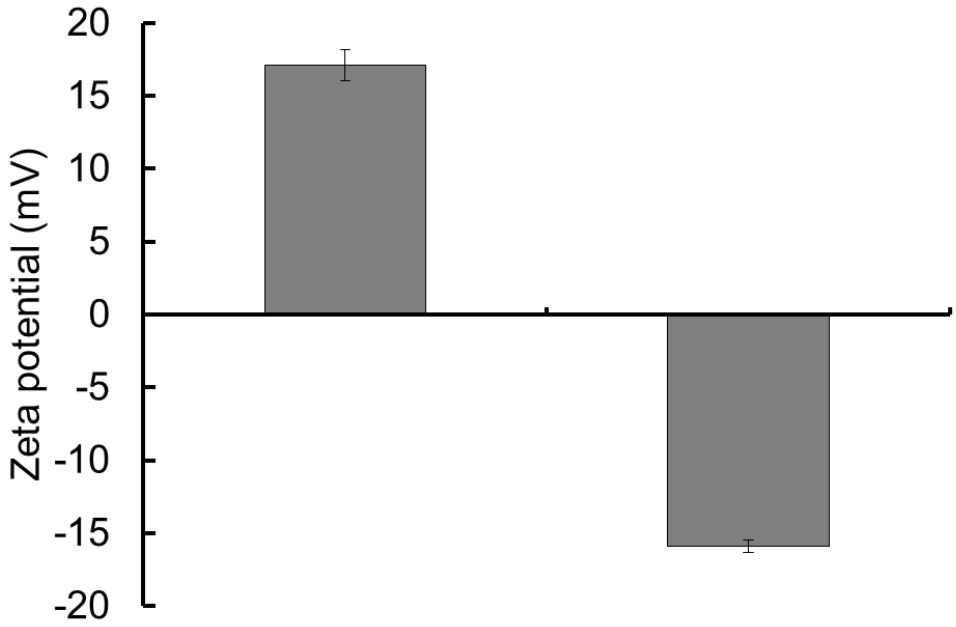

Figure S4 Characterization by Dynamic light scattering at 25 ˚C and pH 7.4 (A) Hydrodynamic diameter of PLL-DDSA-SA (B) Zeta potential of PLL and PLL-DDSA-SA.